Research

Cell Calcium (1999) **26** (6), 271–279

Article No. ceca.1999.0085

Construction of a confocal microscope for real-time *x-y* and *x-z* imaging

N. Callamaras, I. Parker

Laboratory of cellular and Molecular Neurobiology, Department of Neurobiology and Behavior, University of California, Irvine, USA

Summary We describe the construction of a simple 'real-time' laser-scanning confocal microscope, and illustrate its use for rapid imaging of elementary intracellular calcium signaling events. A resonant scanning galvanometer (8 kHz) allows *x-y* frame acquisition rates of 15 or 30 Hz, and the use of mirrors to scan the laser beam permits use of true, pinhole confocal detection to provide diffraction-limited spatial resolution. Furthermore, use of a piezoelectric device to rapidly focus the objective lens allows axial (*x-z*) images to be obtained from thick specimens at similar frame rates. A computer with image acquisition and graphics cards converts the output from the microscope to a standard video signal, which can then be recorded on videotape and analyzed by regular image processing systems. The system is largely made from commercially available components and requires little custom construction of mechanical parts or electronic circuitry. It costs only a small fraction of that of comparable commercial instruments, yet offers greater versatility and similar or better performance. © Harcourt Publishers Ltd 1999

INTRODUCTION

The use of confocal laser-scanning microscopes in conjunction with fluorescent calcium indicator dyes has allowed detailed imaging studies of the spatio-temporal aspects of intracellular calcium signaling. In particular, the high spatial resolution of this technique has contributed greatly to our understanding of the localized elementary release events ('puffs' and 'sparks') that underlie intracellular calcium liberation mediated by inositol trisphosphate- ($InsP_3$) and ryanodine-receptors [1, 3]. A limitation, however, is that the speed of most commercial instruments when used for 2-dimensional (*x-y*) scanning (typically one frame s^{-1}) is insufficient to resolve the dynamics of these intracellular calcium signals. For this reason, many studies have employed a linescan imaging mode, in which the laser spot is repeatedly scanned along a fixed line; offering high temporal resolution (2 ms per scan) at the expense of providing spatial information in only one dimension. Rapid *x-y* imaging, however, remains the ideal. This mode provides a more intuitive view of intracellular calcium events, allows for a much more extensive sampling throughout a plane within a cell rather than along a fixed line, and reduces the inherent uncertainty in linescan imaging as to whether observed events arise focally on the scan line.

In addition to various technical limitations, a further practical difficulty with confocal microscopy is the high purchase cost of the instruments. This can be considerably reduced by those investigators who are willing and able to construct their own microscopes, because the cost of the components represents only a small fraction of the selling price of commercial microscopes. Furthermore, a custom-built microscope can be optimized and readily reconfigured for specific applications, and provide a performance as good or better than commercial instruments. We have previously described the construction of a linescan confocal microscope for study of calcium dynamics [4,5], and now describe a second generation model that permits *x-y* and *x-z* imaging at rates of 15 and 30 frames.

'Real-time' confocal microscopes have been designed based on several, very different scanning mechanisms (see[6] for review). Of these, only four have found widespread application: (i) scanning pinhole disk systems, (ii)

Received 2 August 1999
Revised 13 September 1999
Accepted 13 September 1999

Correspondence to: Dr Ian Parker, Laboratory of Cellular and Molecular Neurobiology, Department of Neurobiology and Behavior, University of California Irvine, CA 92697–4550, USA.
Tel.: +1 949 824 7332; fax: +1 949 824 2447; e-mail: iparker@uci.edu

use of acousto-optic devices (AOD) for rapid *x*-scanning of a laser spot, (iii) slit-scanning systems, and (iv) use of a resonant galvanometer mirror allowing *x*-scanning of a laser spot at video rate (8 kHz). In selecting among these approaches, we considered both their relative technical advantages, and their ease of construction.

A major disadvantage of scanning disk systems is that they generally suffer from very low light throughput, because the pinhole apertures form only a small fraction of the area of the disc. Although a recent design (Ultra VIEW CLSM; EG & G Wallac) overcomes this limitation by addition of a microlens array, this design is impractical for 'home' construction, due to the high tolerances required in fabricating the pinhole and lens discs. Instruments based on use of an AOD are probably the most widely used video-rate confocal microscopes at present (Odyssey and Oz; Noran Instruments Inc.). A fundamental limitation of this design, however, is that the AOD is wavelength dependent, so that fluorescence emission cannot be descanned through the AOD. Instead, a slit aperture (rather than a pinhole) is used for confocal detection, resulting in a somewhat degraded axial resolution and less good rejection of out-of-focus fluorescence. Furthermore, use of an AOD requires complex beam-shaping optics that present a challenge for the individual constructor. Slit-scanning systems (e.g. Insight; Meridian Instruments Inc.) employ a cylindrical lens to expand a laser beam into a line, that is then rapidly scanned across the specimen and viewed through a slit confocal aperture. This design is mechanically simple, and in principle is well suited for custom construction. A major disadvantage, however, is the reduced confocal sectioning ability resulting from use of a slit aperture. Finally, rapid scanning utilizing a resonant galvanometers mirror permits 'true' confocal imaging through a pinhole aperture, together with a simple optical path that maintains the quality of the laser beam. One drawback is that the *x*-scan is sinusoidal, rather than linear, but this complication can be mitigated by appropriate design.

The construction of a video-rate confocal microscope utilizing a resonant scanner has previously been described (the 'UCSD microscope') [6], and served as the basis for a commercial instrument (RCM-8000; Nikon Inc.). While offering excellent performance and great versatility, the UCSD design is, however, dauntingly complex, and the Nikon system was among the most expensive of all commercial confocal systems. In part, the complexities of these microscopes arose because they were designed to produce a standard video signal (RS170) that can be directly stored on regular video recorders and processed by readily available image analysis systems. This limitation has recently been removed following the advent of inexpensive PCI-based computer imaging boards that accept non-standard video signals, and thereby greatly simplify the design of a resonant scanning microscope. We describe here the construction and use of a system that allows 'real-time' confocal imaging with near diffraction-limited resolution. The total component cost (excluding microscope) was <$25 000. Moreover, the system was surprisingly easy to build, and involved less effort than our earlier linescan model [4].

MATERIALS AND METHODS

Microscope design

Overview

Figure 1A shows an overall block diagram of the confocal microscope and image processing systems, while Figure 1B provides a detailed schematic diagram of the optical layout of the scanning system. The heart of the system is the scan head (Fig. 1C), which contains galvanometer-driven mirrors allowing rapid (8 kHz) scanning in the *x*-axis and slower (15 or 30 Hz) scanning in the *y*-axis. Including the laser, the entire optical path mounts within a 2 × 3 foot area of an optical bench, and is constructed using standard 0.5 inch post-mount components. Power supplies and circuit boards are housed in an adjacent rack-mount cabinet. The confocal scanner interfaces through the video (side) port of an Olympus IX50 inverted microscope, and is bolted alongside the microscope on the optical bench. A PC equipped with an acquisition card capable of accepting non-standard video signals is used to reconstruct the confocal image, and a graphics card in the computer provides a standard RS170 video output signal that can be recorded on videotape and processed using an image analysis system hosted by a second computer.

The following sections describe specific details of construction and use of the microscope. Further information is available from the authors upon request. For more general information pertaining to the principles and applications of biological confocal microscopy see [7].

Fluorescence excitation path

Laser light for fluorescence excitation is derived from a multi-line air-cooled argon ion laser (model 150 ALS; Melles Griot Inc. Carlsbad, CA) and directed via a dichroic mirror (DM: 505DCLP, λ = 505 nm; Chroma Technology, Brattleborogh, VT) onto the *y*-mirror of the scan head. A laser line filter (LLF) in the beam path is used to select the desired excitation wavelength (457, 488, or 514 nm), and a rotating polarizer serves as a continuously variable attenuator to set the intensity of the polarized laser emission. A shutter (S1) provides for blanking of the beam, and lens L1 (f = –50 cm) diverges the laser beam so that it overfills the back aperture of the

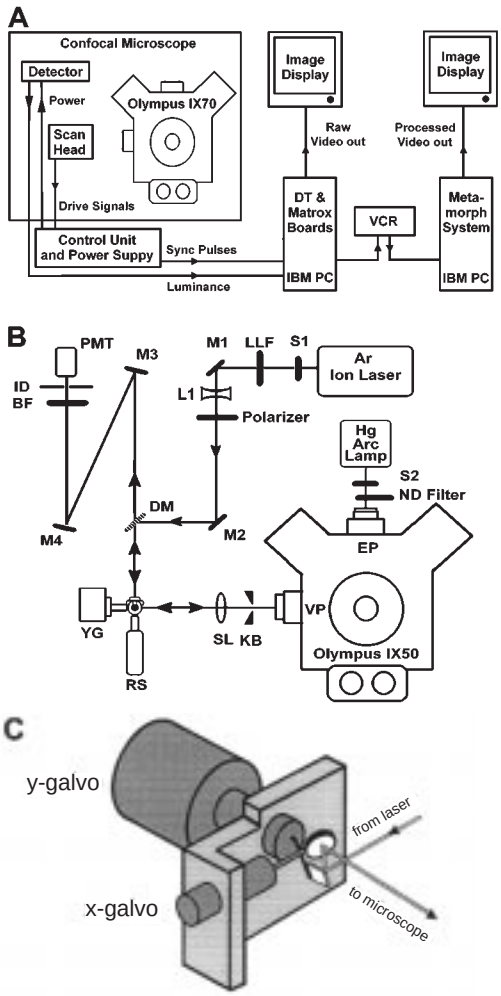

Fig. 1 (A) Overall layout of the confocal system, showing microscope and scan system mounted on an optical bench, rack-mount cabinet containing electronic drive circuits, and computers for image acquisition and processing. (B) Optical schematic of the real-time confocal scanner. The components forming the scan system are mounted on an optical table, and are interfaced through the video port (VP) of an Olympus IX50 inverted microscope. A separate UV flash photolysis system is used for photolysis of caged compounds, and is mounted on the epifluorescence port (EP) of the microscope. S1, S2 = shutters; M1–M4 = fully-reflecting, broadband coated mirrors; DM = dichroic mirror, λ = 500 nm; YG = *y*-scan off-axis scan mirror; RS = resonant scanning mirror; L1 = plano-concave lens, *f* = –50 cm; SL = scan lens, 10x Olympus eyepiece lens; KB = adjustable knife blade aperture; BF = barrier filter, 510 nm long pass; ID = iris diaphragm; PMT = photomultiplier tube (Hamamatsu R-928). (C) Rendering of the scan head assembly.

microscope objective. After deflection through the scan head, the beam is directed through an eyepiece lens (SL; 10X Olympus) mounted at the video port of the microscope, which serves as the scan lens. This is adjusted to be parafocal with the microscope oculars, and the scan head is mounted so that the *x*-scan mirror lies at a conjugate telecentric plane. Changes in angle of the laser beam resulting from rotation of the scan mirrors thus translate to changes in position of the laser spot focused by the scan lens at a conjugate image plane corresponding to the position of the knife-blade aperture, and at the image plane formed in the specimen by the objective lens. Because of the sinusoidal scan of the resonant galvanometer, useful image data are collected only during the central, approximately linear part of the scan. The knife-blade aperture (Coherent Auburn Group, CA) is, therefore, adjusted to blank off the laser beam at the extremes of the scan and thereby minimize bleaching and phototoxicity in the specimen. After passing into the microscope, the laser beam is directed through an 80/20% beam splitter toward the objective lens. Although entailing a 20% loss of light, we find the ability to directly view the scan through the microscope oculars to be invaluable for aligning the microscope and for locating regions of interest. A barrier filter is permanently installed in the binocular head to block laser light from reaching the eyes. Alternatively, the Olympus IX50 can be ordered with a 100/0% beamsplitter to maximize the collection of emitted fluorescence light. The loss of excitation light through the 80/20% beamsplitter is of no consequence, as it can be compensated simply by increasing laser intensity.

Emission path

Fluorescence emitted in the specimen is collected back through the objective lens, and descanned by the mirrors in the scan head to form a stationary beam. This then passes through the dichroic mirror, and appropriate wavelengths longer than the laser excitation are selected by a barrier filter. A long optical path (about 1 m) is used before the confocal aperture so as to provide a large total magnification (~240X), and thus permit the use of an iris diaphragm (Coherent Auburn Group, CA) as a continuously variable aperture. To minimize stray light and to protect the user from exposure to the laser beam, the entire optical path is enclosed by a cover constructed from foam board, painted matte black inside.

Scan head

The scan head (Fig. 1C) contains two orthogonal, galvanometer-driven mirrors to allow rapid (8 kHz) sinusoidal scanning in the *x*-direction, and slower (15 or 30 Hz) scanning in the *y*-direction. This is available as a complete unit (CRS resonant scanner, OATS scanner with off-axis paddle mirror and integral mounting bracket, together with associated circuit boards) from General Scanning Lumonics Inc. Fast *x*-scanning is accomplished by the resonant scanner, which drives a small (2 × 3 mm), elliptical broadband-coated mirror to produce a sinusoidal change in angle. The resonant scanner vibrates at a fixed frequency (set by mechanical resonance), with an amplitude that is stabilized by the driver board. Because

the scanner functions as a rotational analog of a tuning fork, it operates without mechanical wear or backlash. The slower *y*-scan is produced by a second, orthogonal mirror driven by a linear ramp waveform. To minimize geometric errors arising because both mirrors cannot be placed precisely at the same telecentric plane of the microscope, the *y*-scan mirror is mounted on an off-axis paddle arm. Rotation of the *y*-galvanometer thus causes both rotation and translation of the mirror, resulting in a 25-fold reduction in scanning error[8]. Using a 10X eyepiece as the scan lens, the maximum scan angles of the galvanometers provide an imaging field equivalent to approximately one-third of the diameter viewed through the microscope oculars, or about 80 μm with a 40X objective lens.

Detector

Fluorescence light passing through the confocal aperture is detected by a side-on photomultiplier tube (Hamamatsu R-928), which is mounted in a socket including an integral dynode resistor chain and amplifier (Hamamatsu C1053–51). The high voltage for the photomultiplier is derived from a modular power supply (Hamamatsu C2456), providing a stabilized voltage of between 200 and 1100 V. A 10 kΩ potentiometer (VR1) controls the high voltage supply, and hence the gain of the photomultiplier. The photomultiplier anode current is converted to an analog voltage signal by a transimpedance amplifier, and is low-pass filtered at 5 MHz to provide integration of the signal during the pixel dwell time.

Electronics

Figure 2A shows a schematic diagram of the electronics of the confocal scanner, and their connections to the video acquisition board. Very little custom construction is required, as most functions are performed by commercially available circuit boards. The resonant scanner galvanometer is driven by the board supplied by the manufacturer, so that the only external circuitry required is a 10 kΩ potentiometer to set the extent of the mirror excursion. An associated 'daughter' board contains a phase-lock loop and other circuitry that provide a line sync pulse during each cycle of the mirror scan, together with pixel clock pulses to drive the video acquisition board at a non-linear rate so as to compensate for the sinusoidal motion of the mirror (Fig. 2B).

To drive the *y*-scan mirror in synchrony with the resonant *x*-scanner, we constructed a simple-ramp generator circuit, comprising a binary counter and digital-to-analog converter (DAC) (Fig. 2A). Line sync pulses from the resonant scanner are fed into a 12-bit binary ripple counter, which drives a digital-to-analog converter (DAC) to produce a linear ramp voltage. Switch SW1 sets the counter

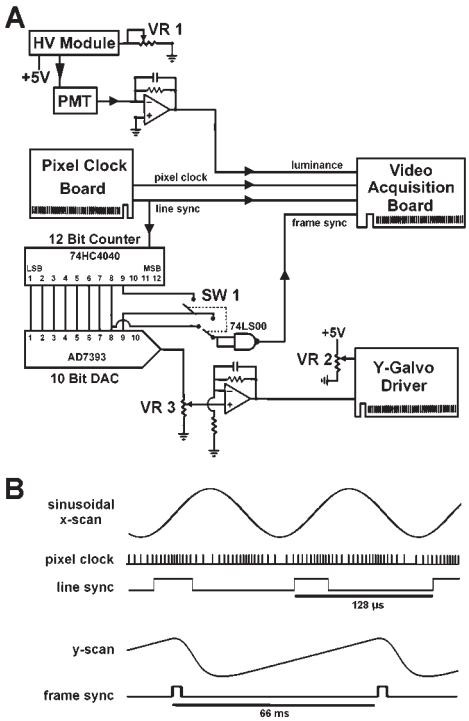

Fig. 2 (A) Electronic drive circuitry and interface to video acquisition card. (B) Waveforms of *x*- and *y*-scan signals, and corresponding sync pulses. Note that the timing of pixel clock pulses is indicated only diagrammatically. All sync pulses are TTL levels.

to increment for either 256 or 512 lines before recycling and outputting a frame sync pulse to the video board, thus allowing for frame rates of 30 and 15 Hz respectively. The output from the DAC is buffered through an amplifier, and filtered with a time constant of 1 ms to smooth out steps in the ramp and flyback signals applied to the *y*-galvanometer. The amplitude of the ramp signal applied to the galvanometer driver board is varied by potentiometer VR3 to set the extent of the *y*-scan, and potentiometer VR2 provides an offset voltage to allow the image area to be panned in the *y*-direction. It is not possible to pan the image in the *x*-direction, because of the resonant mechanism used for rapid *x*-scanning.

x-z imaging

The usual mode of the microscope is for *x*-*y*-*t* imaging (i.e. repeated *x*-*y* scans are obtained with the microscope focused at a fixed confocal plane within the specimen). However, by using a piezoelectric focusing unit (P-721.10; Polytec PI Inc.) to rapidly focus the microscope objective, we are also able to obtain axial images (*x*-*z*) sectioning into the specimen in real time (15 or 30 Hz). In this mode, the output from the *y*-ramp generator is disconnected from the *y*-scan galvanometer, and is instead used as a command signal for the servo electronics dri-

ving the piezo focus unit. Otherwise, the use of the microscope is unchanged, but the vertical dimension of the displayed image now depicts distance into the specimen, rather than displacement in the *y*-direction. Because of mechanical inertia, the focus unit cannot follow rapid step changes in position, and the ramp signal is, therefore, further filtered (time constant = 10 ms) to minimize ringing on the flyback. We had previously described the use of this piezo unit for fast axial line-scan (*z*-*t*) imaging [9], and further details can be found in that paper regarding its use. In particular, precautions are needed to minimize movements of the specimen resulting from transmission of vibrations through the immersion oil.

Image acquisition and storage

To construct images from the luminance and sync signals generated by the confocal scanner, we use a PCI-based video acquisition board capable of accepting non-standard inputs (DT 3152; Data Translation Inc. Marlboro, MA). Use of the board is straightforward. The luminance signal (PMT output), pixel clock, line sync, and frame sync are connected appropriately to the interface cable, and the 'DT-acquire' program provided with the board is set up to allow pass-through of the confocal image to the computer screen. One limitation at present is that the supplied device drivers do not support bi-directional scanning. Thus, data are acquired only as the resonant mirror scans in one direction, and data during the return scan are lost. Nevertheless, full-frame images are acquired at a frame rate of 15 Hz, and faster frame rates can be accomplished by reducing the *y*-resolution (e.g. 30 Hz at about 220 lines of resolution). In the future, we hope to modify the software device driver to allow successive scans to be read into the frame buffer alternately in forward and backward directions; thus giving full-frame resolution at 30 Hz frame rate.

The DT3152 board is able to transfer images in real time to the PC memory but, even with the large amount of RAM now available at modest prices, the ability of computers to store image data is still restricted (e.g. 1 min recording requires about 200 MB). Instead, we use the computer hosting the acquisition board as a video scan converter, to provide a standard (RS170) video output signal that may then be recorded on VHS tape and subsequently re-digitized by a regular image processing system (MetaMorph; Universal Imaging Inc.). This is accomplished using a computer graphics card (Marvel 200 TV; Matrox. Montreal) that provides video outputs (composite and S-video) of the pass-through image displayed on the VGA screen by the DT3152 board. As illustrated in Figure 3, this involves only a slight compromise in spatial resolution and linearity of intensity values. An alternative approach would be to develop software support for non-standard video acquisition by a commercial image processing and analysis system. This would provide optimal fidelity, and allow use of only a single host computer.

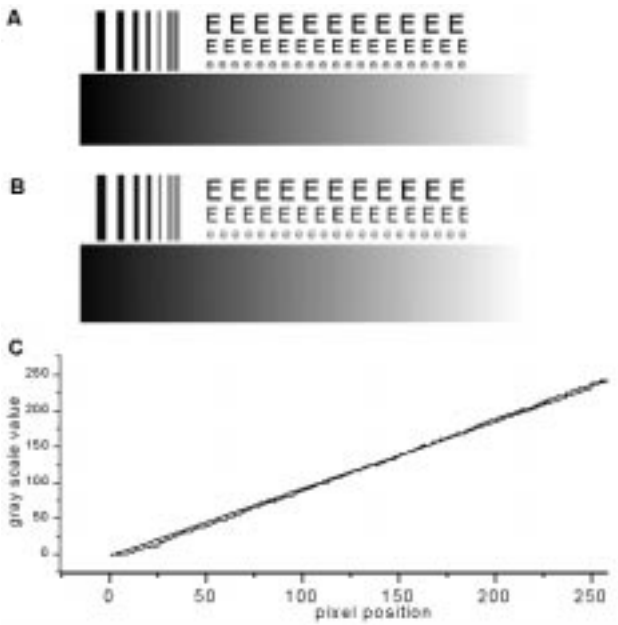

Fig. 3 Fidelity of conversion to video signal, assessed using a test pattern generated using Adobe Photoshop. (A) Original test pattern, before conversion to a video signal. The finest lines in the grid are 1 pixel wide. The grey scale shows linearly increasing intensity values from 0 (black) to 255 (white). (B) The same test pattern, after video conversion through the TV output of the Matrox graphics board, and re-digitization by an image processing system (MetaMorph) hosted by a second computer. (C) Fidelity of intensity values is maintained after video conversion. Plots show measurements of intensity values as a function of pixel position along the grey-scale bars shown in (A) and (B). The smooth line was obtained from the original image, and the slightly jagged line after re-digitization of the video signal.

Operation

Operation of the confocal scanner is accomplished through manual controls in the optical path (accessible through cut-outs in the instrument cover), and electronic controls on the rack-mount cabinet. The laser excitation line (458, 488 or 512 nm) is selected by filters (LLF, Fig. 1B) in a rotating wheel, and a second filter wheel in the emission path (BF; Fig. 1B) is used to select desired emission wavelengths (e.g. 510 nm long-pass, 570 nm long-pass, 510–555 nm band-pass). Determination of the optimal imaging conditions requires a judicious interplay between settings of the confocal aperture, photomultiplier gain, and laser power. Use of a small aperture provides the best axial resolution, though at the expense of reduced light throughput (Fig. 4). This latter effect can be at least partially compensated for by increasing the laser power incident on the specimen (by rotating the polarizer

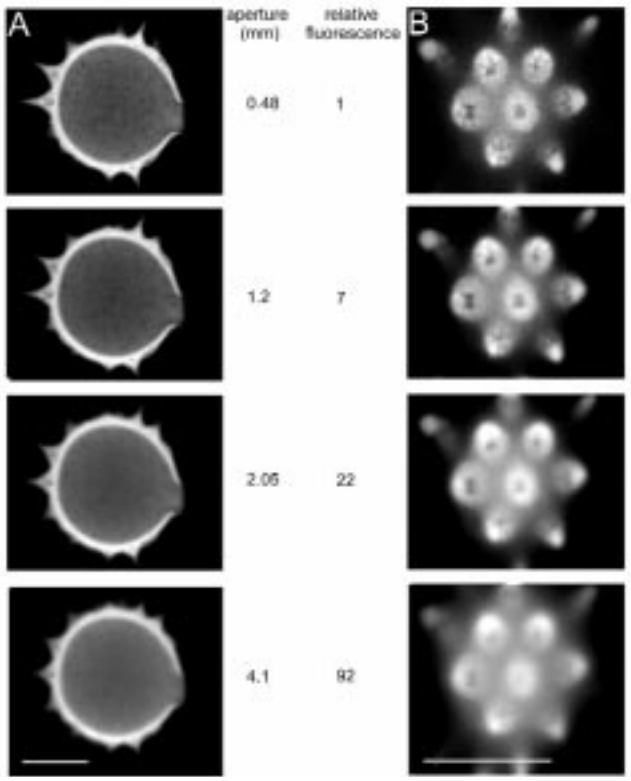

Fig. 4 Spatial resolution and effect of varying confocal aperture. The images show a fluorescent pollen grain (mixed pollen grain slide; Carolina Biological Supply), in which hollow conical 'spikes' protrude from a spherical body. A good test of axial resolution is provided by the ability of the confocal microscope to section through the spikes while rejecting out-of-focus fluorescence from the body. (A) Images obtained at low magnification with the optical section focused through the center of the pollen grain. The sequences of images was obtained using different confocal aperture settings as indicated (in mm). The photomultiplier gain was increased to compensate for the lower signal level at smaller apertures, and images were averaged over 64 scans so that the apparent spatial resolution was not degraded by low photon count rates. (B) Corresponding images at higher magnification, focused just below the body of the pollen grain so as to section through protruding 'spikes'. Calibration bars in (A and B) are 10 μm. Tabulated values of relative fluorescence give the relative intensities at various confocal apertures measured by the photomultiplier at constant laser power while focusing into a droplet of fluoresceine.

in the beam path), but with increased risk of photobleaching and phototoxicity. Alternatively, the photomultiplier gain can be increased to provide a brighter, albeit noisier signal.

The magnification provided by the confocal scanner is determined by the potentiometers that set the amplitude of the sinusoidal *x*-scan and the linear *y*-scan ramp. These are set by 10-turn readout dials, and are calibrated to provide a convenient range of zoom factors (with 1-to-1 aspect ratio) by imaging a stage micrometer. For each zoom setting, the knife-blade aperture (Fig. 1B) is adjusted to blank off the laser beam at the peaks of the sinusoidal *x*-scan where no image data are collected.

Alignment

Initial alignment of the system during construction is facilitated by removing excitation and emission filters, and focusing the microscope on a mirrored slide, so that the paths of both the incident laser beam and the reflected light can readily be visualized by placing a white card in the beam path. The beam from the laser is directed onto the lower paddle mirror in the scan head by appropriate adjustments of M1, M2 and DM (Fig. 1B), and the head assembly is located so that the resonant mirror is at the height of the microscope video port axis. The scan lens is positioned to be parafocal with the image observed through the microscope oculars, and the entire microscope (with attached scan lens) is then moved sideways so that the scan mirrors lie at a conjugate telecentric plane of the microscope. This is most easily determined by removing the microscope objective lens and placing a piece of frosted glass over the opening. With the *y*-mirror scanning slowly (15 Hz) the image of the laser beam on the glass is stationary when the distance from the scan mirrors to the scan lens is correct, but otherwise appears to move. Furthermore, the divergence of the laser beam (set by L1; Fig. 1B) should be sufficient that the beam overfills the back aperture of the objective. Finally, light reflected from the mirrored slide is directed by M3 and M4 (Fig. 1B) to pass through the confocal aperture.

While in use, fine adjustment of mirror M4 provides a convenient means of 'tweaking' the alignment of the confocal aperture, and is set to provide the brightest signal from a fluorescent specimen, with the confocal aperture stopped down to its minimum opening. The mirror is held in a mount with adjusting screws located on the top (TopAdjust mirror mount; Coherent Inc., Auburn, CA), so that this alignment can be done without removing the cover.

Laser safety

The argon ion laser presents a significant eye safety hazard, and the manufacturer's handbook should be consulted for appropriate safety measures. General precautions involve mounting the system so that the laser beam is below eye level, and placing covers over all exposed beams. Because our system is used by only a few, trained personnel, we did not implement the use of interlock microswitches to shut down the laser when covers are removed; but this precaution would be appropriate if a microscope were constructed for shared use.

RESULTS AND DISCUSSION

In this section we describe tests of the microscope resolution, and illustrate its application for imaging subcellular calcium transients. All data were obtained using an Olympus 40X fluorescence objective (oil immersion; numerical aperture 1.35), with excitation by the 488 nm laser line and a 510 nm long-pass barrier filter. Calcium images were obtained from *Xenopus* oocytes, injected to final intracellular concentrations of approximately 40 μM fluo-4 and 5 μM caged InsP_3 [4,5].

Spatial resolution

A convenient measure of the spatial resolution of a confocal microscope is provided by the point spread function, which can be determined as the full-width at half-maximal intensity (FWHM) of fluorescence imaged from sub-resolution beads. Using 100 nm diameter fluorescent beads (FluoSpheres; Molecular Probes Inc, Eugene, OR) in water, and with the confocal aperture at its minimum setting (0.48 mm: equivalent to 0.2 μm at the specimen plane), we measured a lateral FWHM of about 300 nm, and an axial FWHM of about 800 nm. Both of these values are close to that expected for diffraction-limited performance [10]. Figure 4 further illustrates how the axial resolution improves with decreasing size of the confocal aperture. The images show a 'spiky' fluorescent pollen grain: a readily available specimen that provides a good test of the ability of a confocal microscope to section through the protruding, hollow spines while rejecting out-of-focus fluorescence from the body of the pollen grain. With small apertures, the spines are well resolved, and detail is apparent in their walls. The trade-off, however, is the marked decrease in brightness of the signal as the aperture is reduced, as indicated in Figure 4 by the relative light intensities reaching the photomultiplier at various aperture settings. This can be partially compensated for by reducing the attenuation of the laser beam, but we find that intensities greater than about 200 μW (measured at the back aperture of the objective) cause unacceptably rapid bleaching.

Conversion of the image signal from the acquisition board to a standard video signal results in only slight degradation of spatial resolution (Fig. 3). Furthermore, this is of little practical significance because, even at the lowest zoom setting and using a 40 X objective, the image is oversampled such that 1 pixel corresponds to only about 200 nm; less than the diffraction-limited resolution. In terms of dynamic range, photomultipliers provide a signal that is linearly proportional to incident light intensity over a very wide dynamic range. This linearity is subsequently well maintained through the process of conversion to a video signal (Fig. 3C).

Image fidelity

The spatial linearity of the scan in both *x*- and *y*-dimensions was tested by imaging a stage micrometer calibrated in 2 μm increments. The maximum deviation from linearity with pixel position in the final image with maximal scan amplitude (after conversion to a standard video signal and redigitization) was <5 pixels (about 1%) in the *x*-axis, and was within 1 pixel in the *y*-axis. There was no detectable pixel 'jitter' between repeated frames. The evenness of field was checked by imaging into a large volume of fluoresceine. Fluorescence brightness remained uniform throughout the entire field at maximum scan amplitude to within <3.5%.

Imaging of intracellular calcium transients

Our primary motivation in constructing this instrument was to image the elementary calcium puffs that underlie InsP_3-mediated calcium liberation from intracellular stores [1,11]. Photorelease of InsP_3 from a caged precursor provides a convenient means to evoke these signals [12], and the microscope system was, therefore, designed to allow UV photolysis of caged compounds simultaneously with confocal imaging (Fig. 1B). Figure 5 illustrates puffs and repetitive calcium waves evoked in a *Xenopus* oocyte by sustained photorelease of InsP_3. The images in Figure 5A are taken from a video record obtained at 15 frames s^{-1}, and show both discrete puffs arising at several sites, and the subsequent triggering of a propagating calcium wave by a puff arising near the center of the field. The traces in Figure 5B show fluorescence measurements from 2 puff sites, illustrating the appearance of repetitive waves and puffs during a recording period of over 5 min.

Axial imaging of calcium signals

Xenopus oocytes provide a convenient model cell system for study of intracellular calcium signaling, and have contributed greatly to our understanding of calcium waves and elementary events. Unlike the case for small, transparent cells, however, it is difficult to resolve the radial organization of subcellular calcium signals in the large (1 mm diameter) turbid oocyte. To circumvent this problem we use a piezoelectric objective focusing unit [9], in conjunction with the resonant *x*-scanner, to obtain *x*-*z* images of calcium puffs arising in a plane extending into the oocyte. The examples in Figure 6 show puffs originating at two, laterally displaced sites in response to photorelease of InsP_3 uniformly throughout the imaging area. In images A through C, a puff at one site originated a few μm into the cell, and calcium then diffused toward the cell membrane. This ability to obtain time-resolved axial images may be useful not only for subcellular localization within large individual cells, but should facilitate

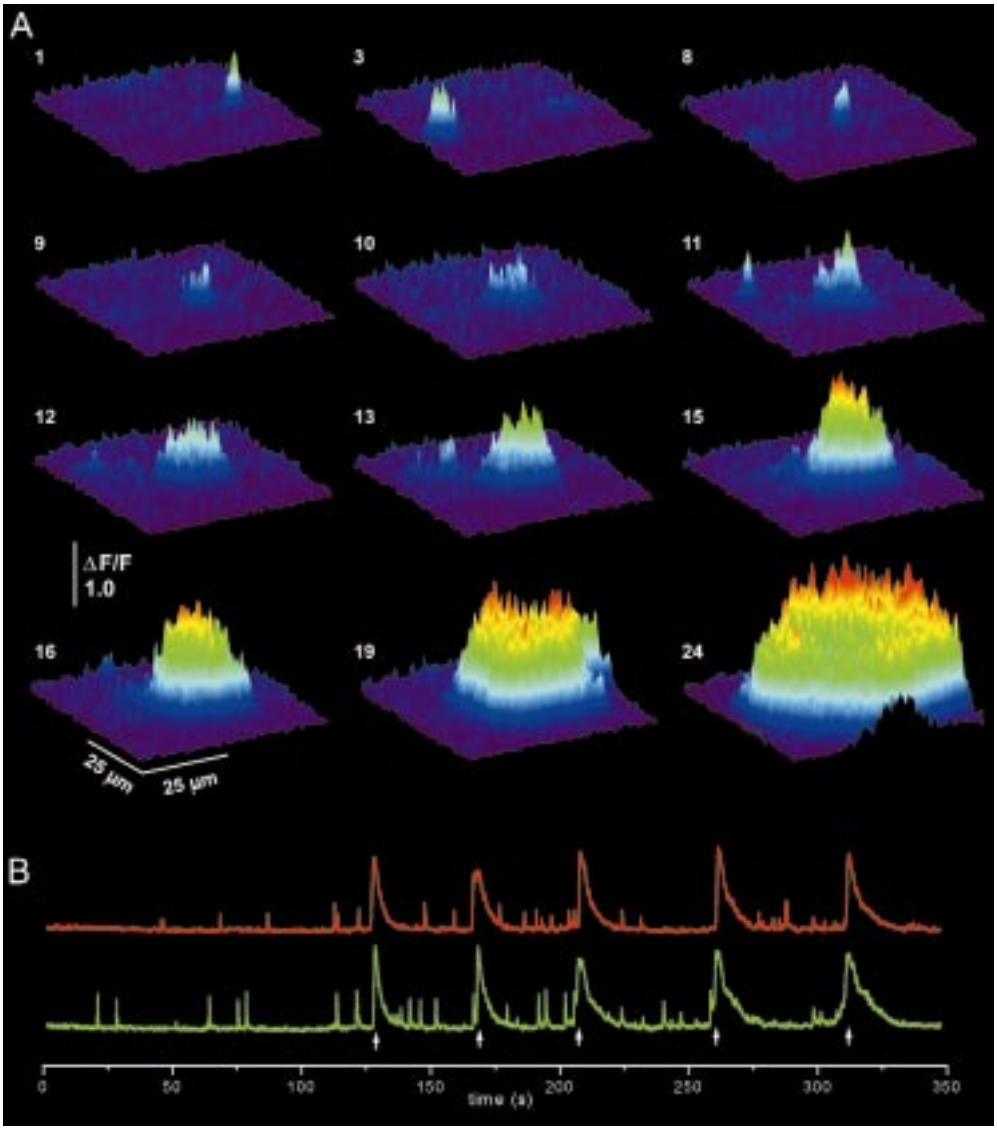

Fig. 5 Calcium puffs and waves imaged in *Xenopus* oocytes by *x-y* scanning. (A) Successive images show selected frames taken from a sequence recorded at 15 frames s^{-1}. Frame numbers are indicated next to each image. The fluorescence at each pixel is expressed as a ratio relative to the average resting fluorescence at that pixel before stimulation, and increasing ratio is depicted both by height of the surface representation and by increasingly 'warm' colors. The oocyte was loaded with fluo-4 and caged InsP_3, and InsP_3 was photoreleased throughout the record. Individual puffs were first observed at several sites throughout the imaging field, and a calcium wave was then triggered by a puff. (B) Records of fluorescence intensity monitored from 6 × 6 pixel regions centered on 2 different puff sites. The oocyte was continuously exposed to low-intensity UV light, so as to cause a roughly constant elevation of [InsP_3]. Periodic calcium waves propagated throughout the imaging field (arrows), interspersed with localized puffs that arose independently at the two sites.

study of dynamic signaling in different cellular layers within thick tissues such as blood vessels.

CONCLUSIONS

This paper describes the construction of a 'real-time' confocal microscope, and its application for imaging intracellular calcium transients. The time resolution of the system (up to 30 frames s^{-1}) is comparable to that of conventional video-fluorescence microscopy, and is adequate for many studies of calcium waves and InsP_3-evoked elementary calcium events, but is probably too slow to satisfactorily resolve the faster calcium sparks in muscle cells. A key feature is the use of mirrors to deflect

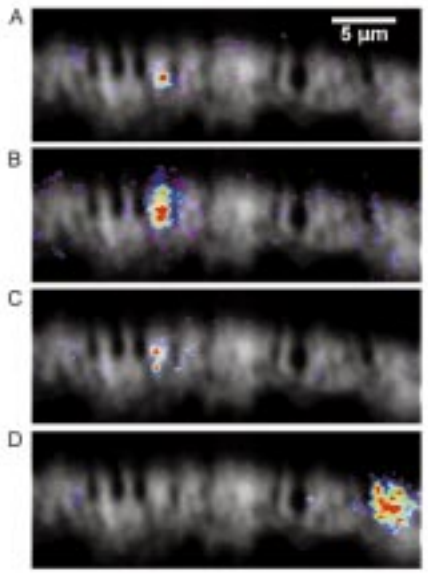

Fig. 6 Axial imaging of calcium puffs in *Xenopus* oocytes. (A–D) Images show individual *x-z* frames, where the vertical dimension depicts distance into the oocyte, with the cell surface uppermost. In each image, the resting fluorescence of fluo-4 loaded into the oocyte is shown in monochrome, to provide an indication of the cytosolic morphology. This signal fades with increasing depth into the cell, due to light scattering in the highly turbid cytoplasm. Circular voids result from the presence of cortical granules. Transient, calcium-dependent increases in fluorescence are depicted by a pseudocolor representation, with increasing $[Ca^{2+}]$ corresponding to increasingly 'warm' colors. The oocyte was stimulated by photoreleasing $InsP_3$ at a concentration that caused the generation of localized calcium puffs. Images in (A–C) show successive frames at intervals of 66 ms, illustrating the spread of calcium from a puff that arose a few μm below the cell surface. The image in (D) shows a puff that occurred at a different site a few seconds later.

the laser beam, with a resonant scanner providing the fast *x*-scan required for video-rate frame imaging. This allows the use of a true pinhole confocal aperture to obtain optimal axial resolution, in contrast to designs using slit scanning or an accousto-optic device for laser scanning, in which the resolution is necessarily degraded by the requirement of a slit confocal aperture. Dual-mirror scanning also has advantages in that the system can be readily adapted to work with UV excitation, as well as for 2-photon imaging using a femtosecond pulsed laser source. The only commercial instrument based on this scanning mechanism (Nikon RCM-8000) cost about $300 000 (including specialized facilities for calcium ratio imaging), and is presently out of production pending introduction of a new model.

Our microscope utilizes existing principles, and our main object is to present a simplified design, based largely on 'off-the-shelf' components, that can be readily constructed by investigators who are not expert in optics and electronics. The cost is no more than that of a good 'wide-field' video fluorescence system, whereas the microscope offers a performance and versatility that is, in many instances, comparable to, or better than, commercially available video-rate confocal systems. Finally, we would point out that further benefits accrue to those who build their own instrument; including a thorough appreciation of the working principles and capabilities of the microscope, as well as the enjoyment and satisfaction gained from following this 'best of physiological traditions' [13].

ACKNOWLEDGEMENTS

We thank Dr J. Kahle for editorial assistance. Financial support was provided by a grant (GM48071) from the NIH.

REFERENCES

1. Parker I, Choi J, Yao Y. Elementary events of $InsP_3$-induced Ca^{2+} liberation in *Xenopus* oocytes: hot spots, puffs and blips. *Cell Calcium* 1996; **20**: 105–121.
2. Bootman M, Niggli E, Berridge MJ, Lipp P. Imaging the hierarchical Ca^{2+} signalling system in HeLa cells. *J Physiol (Lond)* 1997; **499**: 307–314.
3. Cheng H, Lederer WJ, Cannell MB. Calcium sparks: elementary events underlying excitation-contraction coupling in heart muscle. *Science* 1993; **262**: 740–744.
4. Callamaras N, Parker I. A high-resolution, confocal laser-scanning microscope and flash photolysis system for physiological studies. *Cell Calcium* 1997; **21**: 441–452.
5. Callamaras N, Parker I. Construction of a versatile line-scan confocal microscope for physiological recording. *Meth Enzymol* 1999; **307**: 152–170.
6. Tsien RY, Bacskai BJ. Video-rate confocal microscopy. In: Pawley JB (ed.) *Handbook of Biological Confocal Microscopy*. New York, Plenum, 1995; 459–478.
7. Pawley JB (ed.) Handbook of Biological Confocal Microscopy. Plenum, 1995.
8. Stelzer EHK. The intermediate optical system of laser-scanning confocal microscopes. In: Pawley JB (ed.) *Handbook of Biological Confocal Microscopy*. New York, Plenum, 1995; 139–154.
9. Callamaras N, Parker I. Radial localization of inositol 1,4,5-trisphosphate-sensitive Ca^{2+} release sites in *Xenopus* oocytes resolved by axial confocal linescan imaging. *J Gen Physiol* 1999; **113**: 199–213.
10. Wilson T. The role of the pinhole in confocal imaging systems. In: Pawley JB (ed.) *Handbook of Biological Confocal Microscopy*. New York, Plenum, 1995; 167–182.
11. Sun X-P, Callamaras N, Marchant JS, Parker I. A continuum of $InsP_3$-mediated elementary Ca^{2+} signalling events in *Xenopus* oocytes. *J Physiol* (Lond); **509**: 67–80.
12. Callamaras N, Parker I. Caged inositol 1,4,5-trisphosphate for studying release of Ca^{2+} from intracellular stores. *Meth Enzymol* 1998; **291**: 380–403.
13. Eisner DA, Traford AW. A sideways look at sparks, quarks, puffs and blips. *J Physiol (Lond)* 1996; **497**: 2.